Phase transitions in $Al_2(WO_4)_3$: high pressure investigations of low frequency dielectric constant and crystal structure

2004 J. Phys.: Condens. Matter 16 7321

(http://iopscience.iop.org/0953-8984/16/41/013)

INSTITUTE OF PHYSICS PUBLISHING JOURNAL OF PHYSICS: CONDENSED MATTER

J. Phys.: Condens. Matter **16** (2004) 7321–7330 PII: S0953-8984(04)83815-3

Phase transitions in $Al_2(WO_4)_3$: high pressure investigations of low frequency dielectric constant and crystal structure

G D Mukherjee[1], V Vijaykumar[1], S N Achary[2], A K Tyagi[2] and B K Godwal[1]

[1] High Pressure Physics Division, Bhabha Atomic Research Centre, Mumbai 400085, India
[2] Applied Chemistry Division, Bhabha Atomic Research Centre, Mumbai 400085, India

Received 22 July 2004, in final form 23 August 2004
Published 1 October 2004
Online at stacks.iop.org/JPhysCM/16/7321
doi:10.1088/0953-8984/16/41/013

Abstract

Results of the low frequency dielectric constant (ε), dielectric loss and x-ray powder diffraction (XRD) measurements on orthorhombic $Al_2(WO_4)_3$ under pressure are reported. The dielectric constant and the dielectric loss both show a sharp peak at about 0.5 GPa, indicating a ferroelastic phase transformation. This phase is found to be identical to the low temperature monoclinic phase of $Al_2(WO_4)_3$. Another monoclinic modification of $Al_2(WO_4)_3$ is also observed from our XRD studies at 3.4 GPa. $Al_2(WO_4)_3$ amorphizes above a pressure of 18 GPa, and this pressure induced amorphization is attributed to the lack of thermal activation for decomposition.

1. Introduction

$Al_2(WO_4)_3$ belongs to the class of framework structured materials with the basic formula $A_2(BO_4)_3$, where A = Cr, Al, Sc and B = Mo, W. In recent years the above materials have been in the research forefront as they exhibit many interesting physical and chemical properties [1–12]. At ambient conditions these compounds stabilize in a low-density orthorhombic phase with a very flexible framework structure composed of corner sharing polyhedral units. A temperature induced orthorhombic to monoclinic (ferroelastic) phase transformation has been observed in the above materials [1–4]. They are found to be suitable hosts for transition metal and lanthanide ions. Also these materials exhibit unusually high trivalent ion conduction [8–12]. Because of all these features these compounds are useful for many applications, such as in fuel cell electrolytes [13], gas sensors [13], laser materials [2], etc. Most importantly many of the above compounds are found to exhibit negative thermal expansion (NTE) behaviour [3–7]. This remarkable property makes these materials useful as constituents in composites, where the objective is to tune the thermal expansion to a desirable value. Ceramic processing methods and grain interaction stresses in the composites

can produce large changes in local pressures in the material. For practical applications the constituents of the composite should not undergo phase transformations at low pressures. Therefore the high pressure studies of NTE ceramics have assumed a lot of technological importance.

High pressure investigations on the MB_2O_8 and $A_2(BO_4)_3$ (M = Zr, Hf; X = W, Mo, V; A = Sc, Lu, Ho) classes of materials, which show isotropic negative thermal expansion, have revealed the existence of a number of phase changes and amorphization, both reversible and irreversible [13–19]. The NTE behaviour in these materials is attributed to the presence of low frequency rigid modes facilitated by their open network structure with corner linking octahedra and tetrahedra. Theoretical investigations show a close relation between pressure induced amorphization and NTE in these tetrahedrally bonded network structures [20]. Thus the high pressure behaviour of NTE materials is also of significant current interest in basic sciences.

At ambient conditions polycrystalline $Al_2(WO_4)_3$ presents an orthorhombic ($Sc_2(WO_4)_3$-type) structure, which consist of a three dimensional framework of corner linked AlO_6 octahedra and WO_4 tetrahedra. It is one of the rare compounds to exhibit high trivalent Al^{3+} ion conduction [9]. The NTE behaviour of this material observed in dilatometric measurements [21] on sintered samples is not confirmed in x-ray diffraction studies [5]. High pressure high temperature quench experiments have shown that $Al_2(WO_4)_3$ decomposes to $AlWO_4$ and WO_{3-x} at about 5 GPa and 750 °C through an intermediate phase [21]. High pressure ionic conductivity and energy dispersive x-ray diffraction (EDXRD) measurements performed at 400 °C have shown that the crystal structure of $Al_2(WO_4)_3$ undergoes an orthorhombic to tetragonal phase transition at a pressure of about 3 GPa [13]. Our earlier high pressure ac conductivity and compressibility studies on $Al_2(WO_4)_3$ at room temperature have revealed the presence of a reversible phase transition at about 0.5 GPa, where the high pressure phase was predicted to be similar to the low temperature monoclinic phase [22]. Very recently a high pressure Raman scattering study on $Al_2(WO_4)_3$ has indicated the presence of two reversible phase transitions at about 0.28 and 2.8 GPa with the prediction that the intermediate phase is the same as the ambient pressure low temperature monoclinic phase [23].

The low frequency dielectric constant has a direct correlation with the structural behaviour of a solid, and hence the pressure dependence study of this property can give an insight of the underlying physics of transport and lattice dynamical properties. Here we present the measurements of the low frequency dielectric constant (ε) up to 6 GPa in an effort to gather more detailed information about the transition observed in the compound from earlier studies [22, 23]. Also we present the results of the high pressure angle dispersive powder x-ray diffraction (ADXRD) measurements on the orthorhombic phase of $Al_2(WO_4)_3$ up to 18 GPa, which was carried out to investigate the details of the high pressure phase and to check on the possibility of the pressure induced amorphization.

2. Experimental details

$Al_2(WO_4)_3$ was prepared by conventional solid state reaction of Al_2O_3 and WO_3 [21]. The compound was found to be phase pure (JCPDS 24-1101) from powder x-ray diffraction data, which were collected using a Philips PW1710 model diffractometer in the 2Θ range 10°–90° with Ni filtered Cu Kα (Kα_1 = 1.5406 Å and Kα_2 = 1.5444 Å) radiation (see figure 1). The powdered product was made into pellets of 3 mm diameter and 0.25 mm thickness and sintered at 1100 °C to obtain dense pellets for the dielectric measurements. High pressure dielectric measurements were carried out using a Bridgman anvil (BA) apparatus of 12.7 mm face diameter. The cell assembly consisted of two pyrophyllite gaskets of 12.5 mm OD, 3 mm ID

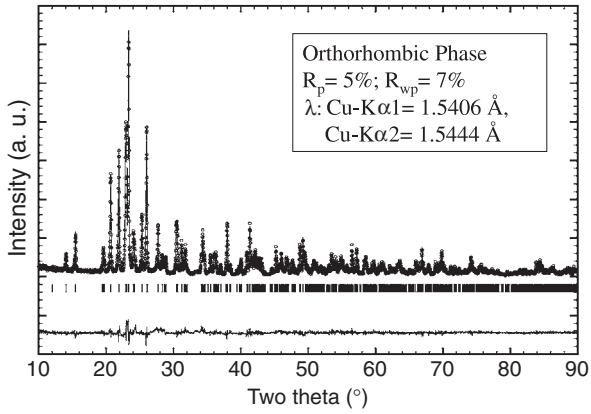

Figure 1. Laboratory ADXRD pattern of orthorhombic $Al_2(WO_4)_3$ using Ni filtered Cu Kα along with the Rietveld refinement fit.

and 0.22 mm thickness and two talc-epoxy discs of 3 mm diameter. The sample was placed in between the two gaskets with one talc-epoxy disc below the sample and the other on the top. The two gaskets contained flattened copper leads. Two copper foils of 0.02 mm thickness and 3 mm diameter were inserted between the copper leads and the sample. The talc-epoxy discs worked as the pressure transmitting medium. The capacitance and the dielectric loss were measured as a function of pressure using a GR 1689 Precision RLC Digibridge. The pressure was determined by calibration of the load applied to the anvils against fixed points (Bi I–II and Yb hcp–bcc transitions at 2.65 and 4 GPa, respectively).

The high pressure angle dispersive powder x-ray diffraction (ADXRD) measurements were carried out at the powder x-ray diffraction beam line of ELETTRA Synchrotron source, Trieste, Italy, using monochromatized x-rays of wavelength 0.729 Å (calibrated with LaB_6). For the high pressure experiments fine powdered samples of orthorhombic $Al_2(WO_4)_3$ were loaded in a Mao–Bell-type diamond anvil cell (DAC), which had been designed and constructed in Bhabha Atomic Research Centre (BARC) [24]. A pair of diamond anvils with almost identical culet diameter of about 400 μm was used in the DAC. A hardened steel gasket with a central hole of diameter 150 μm and thickness 60 μm contained the sample. A mixture of methanol–ethanol (4:1) was used as the pressure transmitting medium. The pressure was determined *in situ* by using Ag powder as the pressure calibrant, with an estimated error of about 0.05 GPa. Images of the powder diffraction rings were collected with a Mar345 image plate detector from MarResearch and read with a resolution of 100 μm $\times$ 100 μm pixel size. Typical exposure times of 20–30 min were employed for the measurements at high pressures. The images were integrated over the entire powder rings using the FIT2D software [25] and converted to the normal 2Θ versus intensity diffraction pattern. The powder patterns obtained were further corrected for the absorption by the diamond anvils.

3. Results and discussion

3.1. Dielectric constant behaviour with pressure

The capacitance, C, at a given pressure, P is given by

$$C(P) = \varepsilon(P)\frac{A(P)}{d(P)}, \tag{1}$$

where A is the area of the copper electrodes, d is the sample thickness and ε is the dielectric constant. From equation (1) $\varepsilon(P)$ can be obtained from $C(P)$ by taking into account the changes in the sample dimensions due to compression. The change in sample dimension with pressure was estimated by employing the high precision pressure dependent bulk modulus values obtained from an earlier piston-cylinder measurement [22]. The dielectric constant (ε) and the dielectric loss ($\tan\delta$) as a function of pressure, under compression and decompression, of polycrystalline $Al_2(WO_4)_3$ are shown in figure 2. It can be seen that both the dielectric constant and loss under compression show a sharp peak at about 0.5 GPa, with values remaining almost constant above 1.0 GPa. The pressure decompression curve shows a small hump around 0.5 GPa. This behaviour of the low frequency dielectric constant at about 0.5 GPa observed in two independent measurements can be attributed to a phase transition induced by pressure. The small hump shown at the transition pressure during decompression is probably due to the complete non-recovery of the orthorhombic phase. Similar anomalies were also observed in the ac conductivity and compressibility studies on orthorhombic $Al_2(WO_4)_3$ [22]. A pressure induced phase transition has been reported from high pressure Raman spectroscopy studies on $Al_2(WO_4)_3$ in the same pressure region [23]. Discontinuities in the slopes of many Raman modes along with softening of some Raman modes below transition pressures are observed [23].

$Al_2(WO_4)_3$ has been found to show a phase transition from the orthorhombic phase at ambient pressure to a monoclinic ferroelastic phase at about 210 K with the framework collapse accompanied by a very small decrease in volume [2]. Since the density of orthorhombic and monoclinic $Al_2(WO_4)_3$ is 5.103 and 5.172 gm cm^{-3} respectively, it is probable that the orthorhombic phase transforms to the monoclinic phase with a small density increase under pressure. This transition has been confirmed by *in situ* x-ray diffraction measurements performed at various pressures and will be discussed in the next section. The anomalous ε behaviour of $Al_2(WO_4)_3$ may also be understood based on such a structural transition, as described below.

At low frequencies the only significant contribution to the dielectric constant comes from the ionic polarizability, which has a direct correlation to the lattice properties of the material. As the pressure increases, orthorhombic $Al_2(WO_4)_3$ goes to a denser phase with a very small volume change by the distortion of flexible Al–O–W bonds. As a result of this the ionic polarization of the compound is affected at the transition, and this is reflected in the anomalous behaviour of both the dielectric constant and dielectric loss at about 0.5 GPa.

The restoring force opposing the lattice distortion vanishes as the phase transition is completed. This should give rise to a soft mode whose polarization vectors describe precisely the lattice distortion taking place in the compound. Since the distortion leads to a net dipole moment due to a relative displacement between the ions, the mode is a transverse optical mode. As the relative displacements of the ions are large close to the transition, the anharmonic terms will be substantial, and the soft mode corresponding to the distortion will be strongly damped. This will show up as a disappearance of a low frequency transverse optical mode in the compound as the pressure corresponding to the phase transition is approached, as has been observed in the Raman spectroscopy studies [23]. As a result the low frequency dielectric constant is expected to diverge at the transition pressure, which is a characteristic of a ferroelastic transition. This result below the phase transition pressure can be checked by indirectly calculating the Grüneisen parameter Γ of the low frequency soft mode. In an ionic crystal, the Lyddane–Sachs–Teller equation describes the relation between the transverse optical mode frequency and the low frequency dielectric constant of the crystal. Under this assumption one can calculate Γ of the optical mode, which is given by

$$\Gamma = \frac{-B_0}{2}\left(\frac{\mathrm{d}\ln\varepsilon}{\mathrm{d}P}\right)_{P=0}. \tag{2}$$

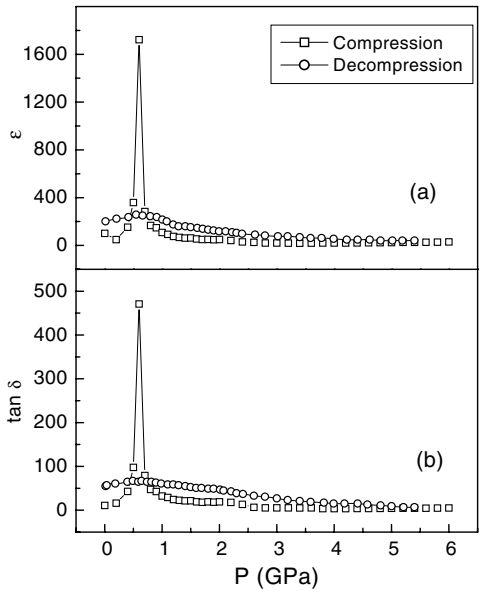

Figure 2. Pressure dependence of (a) the dielectric constant (ε) and (b) dielectric loss ($\tan\delta$) of polycrystalline $Al_2(WO_4)_3$. The symbols represent data obtained under compression (□) and decompression (○).

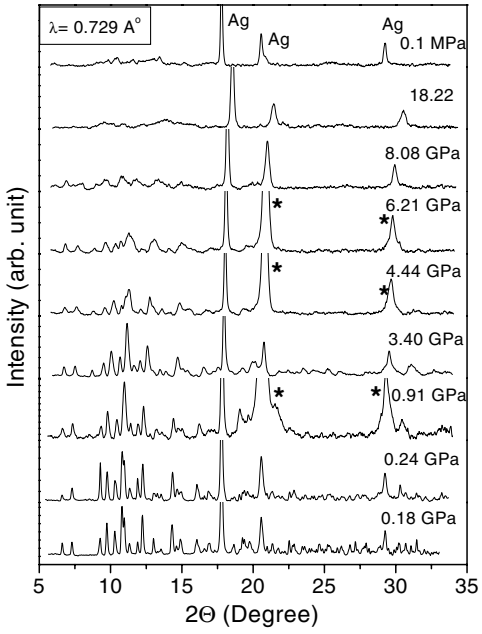

Figure 3. Typical ADXRD patterns of $Al_2(WO_4)_3$ with Ag pressure calibrant under pressure along with the pattern of the pressure released sample (topmost pattern). The symbol (∗) denotes the gasket line along with the pressure calibrant lines.

Substituting for B_0 [22] from our experimental results we get $\Gamma = -22$. In our earlier compressibility study on $Al_2(WO_4)_3$, only a slope change was seen in the pressure evolution of the sample volume across the transition [22]. Therefore this large negative value of Γ indicates that a very small decrease in the volume of the compound produces a relatively large reduction in the optical phonon mode, which in turn induces a considerable change in the dielectric constant. Thus our dielectric constant and dielectric loss measurements are consistent with earlier high pressure data on $Al_2(WO_4)_3$ and indicate an orthorhombic to a ferroelastic monoclinic phase transition at 0.5 GPa.

3.2. ADXRD studies

To confirm the presence of the phase transition at 0.5 GPa and also to identify the new phase, *in situ* high pressure ADXRD measurements were performed at the ELETTRA synchrotron source. Typical x-ray powder patterns collected up to 18 GPa and the pattern after pressure release are shown in figure 3.

The powder diffraction pattern collected under ambient conditions was indexed to the orthorhombic phase with lattice parameters $a = 12.601(3), b = 9.064(2)$ and $c = 9.144(2)$ Å, which is in excellent agreement with the literature values [2]. The structural refinement of the laboratory pattern with the atomic position parameters obtained from single crystal x-ray diffraction studies as given in literature [2] was initiated using GSAS [26] along with a pseudo-Voigt profile function and shifted Chebyshev background function. The final refinement yielded a fit (figure 1) with the value of the residuals $R_p \sim 5\%$, $R_{wp} \sim 7\%$. The refined

Table 1. The atomic position parameters obtained from the Rietveld refinement of the powder ADXRD pattern obtained under ambient condition are compared with those (in italics) obtained from Rietveld refinement of the powder ADXRD pattern measured at 0.18 GPa. The values of the residuals obtained from the structural fits of the ambient pattern are $R_p = 5\%$ and $R_{wp} = 7\%$ and those obtained from the fits of the 0.18 Pa pattern are $R_p = 3\%$ and $R_{wp} = 4\%$.

Atom	x/a	y/b	z/c
W1	0.0000(0)	0.4749(3)	0.2500(0)
	0.0000	*0.4728*	*0.2500*
W2	0.3556(2)	0.3958(2)	0.1178(2)
	0.3575	*0.3944*	*0.1199*
Al	0.3803(9)	0.2512(15)	0.4704(12)
	0.3641	*0.3015*	*0.5002*
O1	0.1429(17)	0.0884(10)	0.0863(19)
	0.0449	*−0.2308*	*0.0385*
O2	0.0677(13)	0.3599(19)	0.1243(20)
	0.1594	*0.5751*	*0.3187*
O3	0.2624(13)	0.3102(19)	−0.0017(18)
	0.4601	*0.4615*	*0.5825*
O4	0.4013(11)	0.0770(18)	0.3372(19)
	0.4026	*0.1154*	*0.3314*
O5	0.4743(10)	0.3201(20)	0.0623(19)
	0.3062	*0.1939*	*0.0479*
O6	0.3278(15)	0.3642(20)	0.3071(11)
	0.4936	*0.3501*	*0.0920*

atomic position parameters (table 1) and bond distances are found to be in good agreement with those previously published [2].

The high pressure ADXRD patterns were indexed using the auto-indexing program DICVOL91 [27] embedded in the CRYSFIRE suite [28]. The pattern at 0.18 GPa could be indexed to the ambient orthorhombic phase with the lattice parameters $a = 12.607(3)$, $b = 9.054(2)$, $c = 9.126(2)$ Å. The structural refinement of the ADXRD pattern obtained at 0.18 GPa was then initiated using the GSAS software by using a suitable model with the lattice parameters obtained from the auto-indexing program [27] and the atom position parameters obtained from the Rietveld refinement of the power pattern taken under ambient condition. Initially the refinement of all non-structural parameters like the background (shifted Chebyshev background function), profile coefficients (pseudo-Voigt profile function) and lattice parameters was carried out using the Le Bail structureless refinement method. Then the structural refinement was initiated with the atomic position parameters obtained from the fit of the ambient powder pattern. But we were unable to obtain a good fit with proper intensity match. In the structure of $Al_2(WO_4)_3$ the nearly rigid WO_4 tetrahedra are more tightly bound to the AlO_6 octahedra due to significantly shorter and more covalent Al–O bonds. As a result the compression of the material in the low pressure region takes place mainly by the rotations and/or tilts of the nearly rigid WO_4 tetrahedra. This is also indicated in the high pressure Raman study [23]. Keeping the above fact in mind the structural refinement of the 0.18 GPa ADXRD pattern was initiated by defining the rigid bodies of tetrahedra [26] and allowing them to rotate. After obtaining a reasonably good fit, for the final stages of refinement the rigid body constraint was removed and replaced with soft bond constraints [26] on the W–O and Al–O bond distances. Figure 4 shows the excellent refinement of the data obtained at 0.18 GPa pressure with values of the residuals $R_p = 3\%$ and $R_{wp} = 4\%$. The new atomic position values are compared with the atomic position parameters obtained from the Rietveld

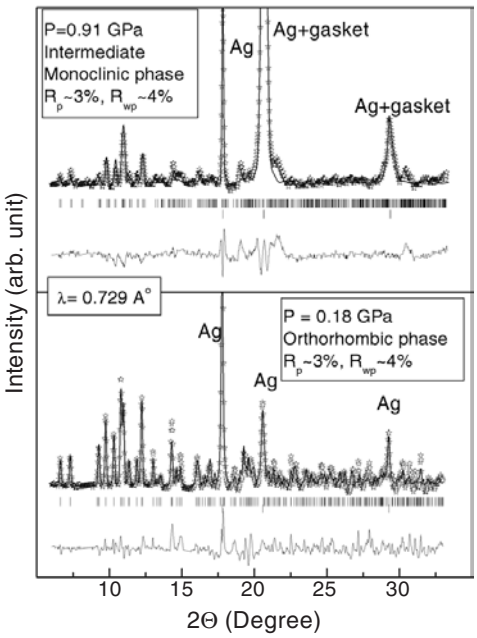

Figure 4. The Rietveld refinement fit of the powder ADXRD patterns at 0.18 GPa (orthorhombic phase) and at 0.91 GPa (intermediate monoclinic phase) along with the difference.

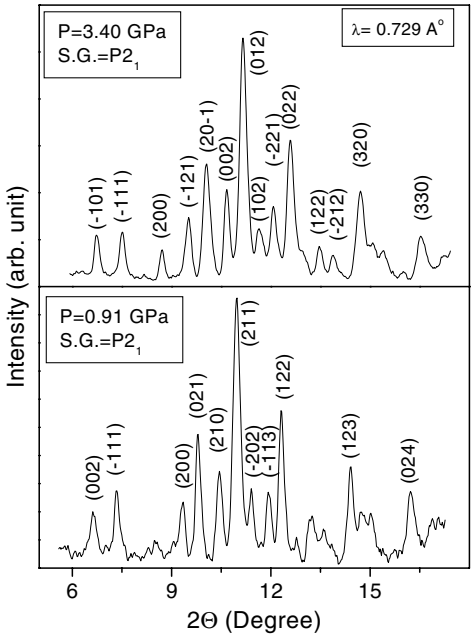

Figure 5. A comparison of the first few lines of the ADXRD patterns of the intermediate pressure monoclinic phase with the high pressure monoclinic phase.

refinement of the ambient powder pattern in table 1. The fitted atomic position parameters and the calculated bond lengths show that in addition to the rotations, the polyhedra are also getting deformed by application of pressure.

The first 21 lines of the ADXRD pattern obtained at 0.91 GPa were indexed using the auto-indexing programs TREOR [29] and DICVOL91 [27] linked in the CRYSFIRE suite [28]. A monoclinic solution very close to the original orthorhombic lattice was suggested with a high figure of merit $M(21) = 17$. The lattice parameters obtained were further refined using the CELREF program [30], which gave the values of the refined lattice parameters $a = 8.954(2)$, $b = 9.074(2)$, $c = 12.592(6)$ Å, and $\beta = 90.51(5)^\circ$, with a cell volume of 1023.1(3) Å^3 (volume reduction $\sim 2\%$). From the systematic absences the best space group was identified as $P2_1$. The lattice parameters obtained from the ADXRD pattern at 0.91 GPa are in excellent agreement with the reported monoclinic cell that was obtained below 210 K [2]. Therefore the structural refinement of the 0.91 GPa ADXRD pattern was initiated using indexed lattice parameters and with the atomic position parameters [2] of the low temperature monoclinic cell. An excellent fit (with $R_p \sim 3\%$ and $R_{wp} \sim 4\%$) was obtained for the space group $P2_1$ (figure 4). This confirms our earlier predictions as well as the results of the high pressure Raman studies that the orthorhombic $Al_2(WO_4)_3$ transforms to a monoclinic lattice with a very small volume change, which is equivalent to the low temperature monoclinic cell of $Al_2(WO_4)_3$.

A careful inspection of the ADXRD pattern obtained at 3.4 GPa showed some changes with respect to the previous pattern, with a new line appearing at low angles. This is clearly seen in figure 5, where a comparison of the intermediate monoclinic phase and the high pressure monoclinic phase is shown up to a 2Θ value of about 18°. The first 20 lines of the powder pattern

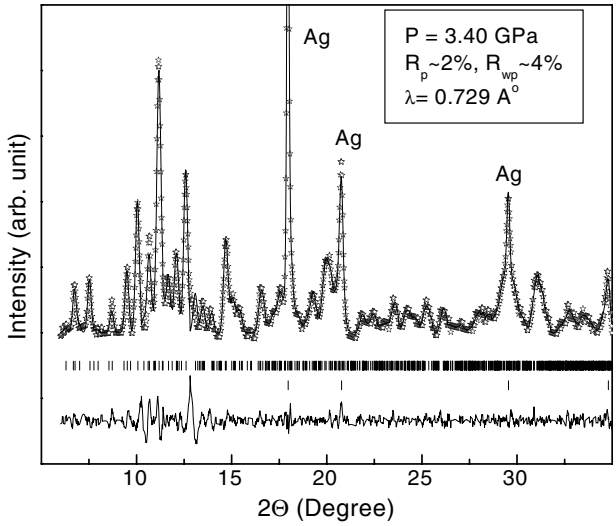

Figure 6. The structureless Le Bail refinement fit of the powder ADXRD pattern at 3.40 GPa (high pressure monoclinic phase) along with the difference.

were then indexed using the CRYSFIRE suite [28], which suggested a different monoclinic solution with a figure of merit $M(20) = 12$. The lattice parameters obtained were further refined using the CELREF program, which gave the values of the refined lattice parameters $a = 9.5929(16), b = 12.5182(30), c = 7.8415(8)$ Å, and $\beta = 91.992(16)°$, with a cell volume of 941.08(29) Å^3. From the systematic absences the best space group suggested was $P2_1$. The cell volume obtained at 3.4 GPa is about 9.6% less than the original orthorhombic cell. The above volume reduction agrees well with our earlier compressibility results where the volume reduction at 3 GPa is about 8.2% of the original volume [22]. The structural refinement of the above phase could not be carried out due to the absence of a proper starting model with correct atomic position parameters. But a refinement of all the non-structural parameters was carried out on our powder ADXRD pattern with shifted Chebyshev background function, pseudo-Voigt profile function and the lattice parameters using the Le Bail structureless refinement method to check the space group and the indexed lattice parameter values (figure 6).

The presence of weak structural changes in $Al_2(WO_4)_3$ above 2.8 GPa was detected in the recent high pressure Raman studies by Maczka *et al* [23]. The above transition is attributed to slight structural changes due to the rotations/tilts of the WO_4 polyhedra [23]. In fact in our earlier compressibility measurement [22] this has been detected as an upturn in the compressibility curve above about 3 GPa. Therefore it can be inferred that the new monoclinic lattice of $Al_2(WO_4)_3$ obtained from our high pressure ADXRD studies at 3.4 GPa is due to the rotations/tilts of the tungstates accompanied by weak changes in the W–O bond lengths and O–W–O bond angles. But the structural refinement could not be initiated on this new phase due to the non-availability of any good model and also because of broadening of the x-ray lines.

From figure 3, the comparison of the pressure evolution of the ADXRD patterns shows a gradual amorphization of $Al_2(WO_4)_3$ starting at about 6 GPa with the sample lines broadening and merging with background with increasing pressure. A careful inspection of the powder patterns shows that with application of pressure the line-broadening is initiated from the lines corresponding to low d values. A complete amorphization is observed at about 18 GPa. The

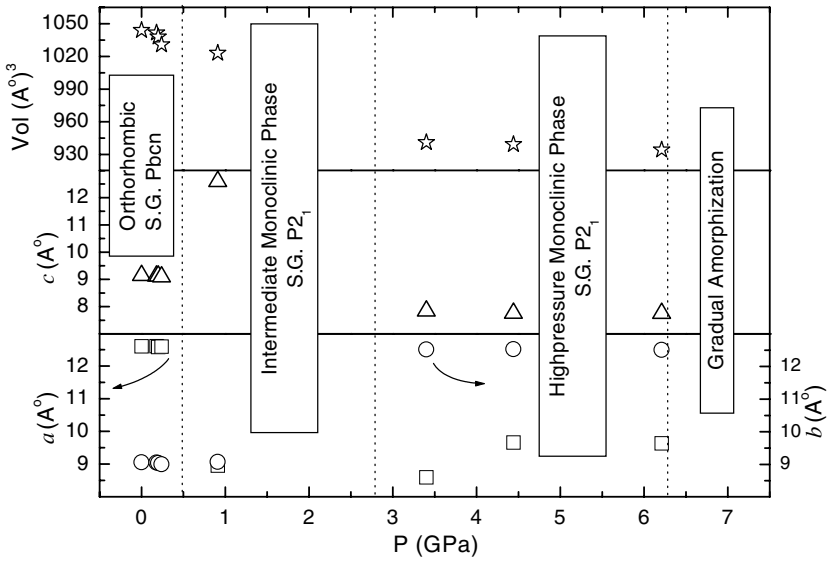

Figure 7. The pressure variation of the lattice parameters and the unit cell volume of $Al_2(WO_4)_3$. The vertical dotted lines show the approximate boundaries among various phases.

absence of any sample lines in the powder pattern of the pressure released sample show that the pressure induced amorphization in $Al_2(WO_4)_3$ is irreversible. Earlier we have seen that orthorhombic $Al_2(WO_4)_3$ decomposes to $AlWO_4$ and WO_{3-x} with a partial oxygen loss when heat treated above 900 °C at a pressure of 5 GPa [21]. Hence it can be inferred that the pressure induced amorphization observed in $Al_2(WO_4)_3$ is due to the kinetic hindrance to decomposition to its daughter compounds, $AlWO_4$ and WO_{3-x}.

In figure 7 the pressure evolution of the lattice parameters and the unit cell volume is shown. The dotted lines show the approximate phase boundaries among various phases determined from the present work and other previous experimental evidences [22, 23]. When going from the orthorhombic to the ferroelastic intermediate monoclinic phase, even though the volume change is minimal, the lattice parameters a and c do show large changes. The second transition from the intermediate monoclinic to the high pressure monoclinic phase takes place with large changes in the b- and c-axes. The above ADXRD results corroborate the observation of slight slope changes in the dielectric constant and the dielectric loss at about 2.6 GPa.

4. Conclusion

We have performed dielectric constant, dielectric loss, and ADXRD measurements on $Al_2(WO_4)_3$ both under pressure compression and decompression at ambient temperature. Our high pressure dielectric measurements confirm the presence of a ferroelastic phase transition induced by pressure in $Al_2(WO_4)_3$ at about 0.5 GPa. We associate the softening of a low frequency optical mode to the phase transition, and the value of the Grüneisen constant of the optical phonon mode is calculated to be $\Gamma = -22$, which is quite large. The ADXRD studies confirm that the phase above 0.5 GPa is of monoclinic symmetry, which is identical to the low temperature monoclinic phase. The new phase obtained at 3.4 GPa could be indexed to a different monoclinic lattice with space group $P2_1$. These phase transitions in $Al_2(WO_4)_3$ under pressure could be attributed to the rotations/tilts of the tungstates. On further compression it amorphizes gradually. The kinetic hindrance to decomposition is the reason

for the pressure induced amorphization. Thus in general, pressure induced amorphization falls into two categories: one with kinetic hindrance to decomposition as in the present case and another with kinetic hindrance to bond reconstruction as in the case of $NbOPO_4$ [31].

Acknowledgments

The authors gratefully thank Dr A Lausi, Dr E Busetto and the ELETTRA users' office for extending all possible cooperation for performing the high pressure ADXRD measurements on $Al_2(WO_4)_3$. These experiments were performed in the spare time during the scheduled period of the proposal no. 2002087.

References

[1] Sleight A W and Brixner L H 1973 *J. Solid State Chem.* **7** 172
[2] Hanuja J, Maczka M, Hermanowicz K, Andruszkiewicz H and Pietraszko A 1993 *J. Solid State Chem.* **105** 49
[3] Evans J S O and Mary T A 2000 *Int. J. Inorg. Mater.* **2** 143
[4] Tyagi A K, Achary S N and Mathews M D 2002 *J. Alloys Compounds* **339** 207
[5] Evans J S O, Mary T A and Sleight A W 1997 *J. Solid State Chem.* **133** 580
[6] Evans J S O, Mary T A and Sleight A W 1998 *Physica* B **241–243** 311
[7] Evans J S O, Mary T A and Sleight A W 1998 *J. Solid State Chem.* **137** 148
[8] Imanaka N, Tamura S, Adachi G and Kowada Y 2000 *Solid State Ion.* **130** 179
[9] Imanaka N, Kobayashi Y, Tamura S and Adachi G 1998 *Electrochem. Solid-State Lett.* **1** 271
[10] Imanaka N, Tamura S, Kobayashi Y, Okazaki Y, Hiraiwa M, Ueda T and Adachi G 2000 *J. Alloys Compounds* **303/304** 303
[11] Okazaki Y, Ueda T, Tamura S, Imanaka N and Adachi G 2000 *Solid State Ion.* **136/137** 437
[12] Secco R A, Liu H, Imanaka N, Adachi G and Rutter M D 2002 *J. Phys. Chem. Solids* **63** 425
[13] Liu H, Secco R A, Imanaka N, Rutter M D, Adachi G and Uchida T 2003 *J. Phys. Chem. Solids* **64** 287
[14] Liu H, Secco R A, Imanaka M and Adachi G 2002 *Solid State Commun.* **121** 177 and references therein
[15] Muthu D V S, Chen B, Wrobel J M, Anderson A H K, Carlson S and Kruger M B 2002 *Phys. Rev.* B **65** 064101
[16] Chen B, Muthu D V S, Liu Z X, Sleight A W and Kruger M B 2001 *Phys. Rev.* B **64** 214111
[17] Evans J S O, Hu Z, Jorgensen J D, Argyriou D N, Short S and Sleight A W 1997 *Science* **275** 61
[18] Perottoni C A and da Jornada J A H 1998 *Science* **280** 886
[19] Paraguassu W, Maczka M, Souza Filho A G, Freire P T C, Mendes Filho J, Melo F E A, Macalik L, Gerward L, Staun Olsen J, Waskowska A and Hanuza J 2004 *Phys. Rev.* B **69** 094111
[20] Speedy R J 1996 *J. Phys.: Condens. Matter* **8** 10907
[21] Achary S N, Mukherjee G D, Tyagi A K and Vaidya S N 2002 *J. Mater. Sci.* **37** 2501
[22] Mukherjee G D, Achary S N, Tyagi A K and Vaidya S N 2003 *J. Phys. Chem. Solids* **64** 611
[23] Maczka M, Paraguassu W, Souza Filho A G, Freire P T C, Mendes Filho J, Melo F E A and Hanuza J 2004 *J. Solid State Chem.* **177** 2002
[24] Vijaykumar V and Meenakshi S 2000 *BARC Technical Report* LISD, BARC, Mumbai
[25] Hammersley A 1998 *FIT2D V10.3 Reference Manual V4.0* ESRF, Grenoble, France
[26] Larson A C and von Dreele R B 1994 *'LANCE'* Los Alamos National Laboratory, Los Alamos, NM
Dollase W A 1986 *J. Appl. Crystallogr.* **19** 267
[27] Boultif A and Louër D 1991 *J. Appl. Crystallogr.* **24** 987
[28] Shirley R 2002 *The Crysfire 2002 System for Automatic Powder Indexing: User's Manual* (Guildford: The Lattice Press)
[29] Werner P-E, Eriksson L and Westdahl M 1985 *J. Appl. Crystallogr.* **18** 367
[30] Altermatt U D and Brown I D 1987 *Acta Crystallogr.* A **34** 125
[31] Mukherjee G D, Vijaykumar V, Godwal B K, Achary S N, Tyagi A K, Lausi A and Busetto E 2003 *ELETTRA HIGHLIGHTS 02-03* p 38